Design of a Broadband Cosecant Squared Pattern Reflector Antenna Using IWO Algorithm

Aliakbar Dastranj, Habibollah Abiri, and Alireza Mallahzadeh

***Abstract*—A cosecant squared pattern reflector antenna fed by a pyramidal double-ridged horn for 2–18 GHz is presented. Invasive weed optimization (IWO) algorithm is used for synthesizing the point source doubly curved reflector antenna. IWO method makes antenna synthesis flexible to achieve extra desired features such as low side lobe level (SLL) and low ripples in the shaped beam region. The simulation results via FEKO software package further prove the validity and versatility of this technique for solving reflector synthesis problems. In addition, experimental investigations are conducted to understand the complete reflector antenna system behaviors. Good agreement between the simulation and measurement has been achieved. The ripple in the cosecant squared region and the SLL is less than 1.5 dB and −25 dB, respectively. Based on the obtained results, the proposed reflector antenna can be used in broadband surveillance-search radar systems.**

***Index Terms*—Cosecant squared pattern, GO method, IWO algorithm, pattern ripple, reflector antenna.**

I. Introduction

Cosecant squared pattern reflector antennas are frequently used in air-surveillance radar systems, where the radiation pattern of the antenna compensates for the free-space loss. The radiation characteristics of the tracking antenna system at the ground control station play a significant role for accurate tracking of an airborne target. Doubly curved reflector antenna is an excellent antenna for achieving cosecant squared pattern in elevation and pencil beam in azimuth plane [1]–[4].

The synthesis procedure on the basis of geometrical optics (GO) method has been described in details by many authors [5]–[8]. Different analysis methods for computing far-field patterns of the doubly curved reflector antennas have been presented [9]–[11]. Various optimization techniques have been used in solving antenna problems. In [12] using genetic algorithm an offset reflector antenna is optimized. An ultra-wideband monopole antenna optimized by means of simulated annealing algorithm and finite element method is presented in [13]. Stochastic optimization of a patch antenna is performed in [14].

IWO is an efficient and robust optimization algorithm in finding global optimum [15] and has been used in antenna design problems [16]–[19]. In [20] IWO algorithm is employed to design a narrowband reflector antenna at 9.37 GHz.

In this communication a cosecant squared pattern reflector antenna fed by a pyramidal double-ridged horn for 2–18 GHz is presented. Based on GO analysis, IWO algorithm is employed for synthesis and optimization of the reflector antenna. A few parameters describe the vertical section curvature of the reflector surface at its center. The goal is optimize these parameters to attain the desired performance which is basically a pattern with low ripples in the cosecant squared region and low SLL. Simulation results have been verified experimentally and excellent agreement is obtained. Finally, the designed reflector using IWO method, using common GO method without optimization, also with physical optics based software TICRA are compared to show the improved performance of the design using IWO method.

Manuscript received June 27, 2012; revised February 16, 2013; accepted March 09, 2013. Date of publication March 22, 2013; date of current version July 01, 2013.

A. Dastranj and H. Abiri are with the School of Electrical and Computer Engineering, Shiraz University, Shiraz 7134851154, Iran (e-mail: abiri@shirazu.ac.ir).

A. Mallahzadeh is with the Electrical Engineering Department, Shahed University, Tehran 1598774811, Iran.

Color versions of one or more of the figures in this communication are available online at http://ieeexplore.ieee.org.

Digital Object Identifier 10.1109/TAP.2013.2254439

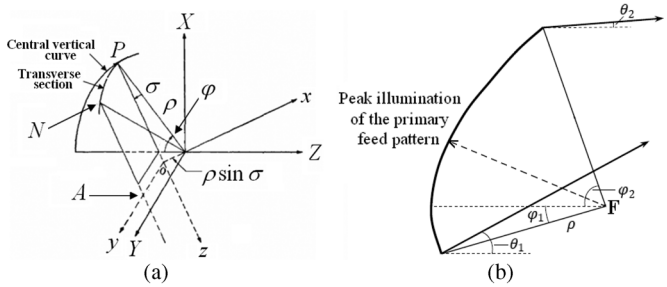

Fig. 1. (a) Ray path in the transverse section curve, (b) General arrangement of the central curve and the feed.

II. Antenna Basics

Antennas with principal plane pattern proportional to the square of the cosecant of the elevation angle have application in target-seeking radar systems. They are also useful in ground-mapping radars and airport beacons [7].

A 2–18 GHz pyramidal double-ridged horn (DRH) antenna is used to illuminate the shaped reflector. The detailed design procedure of the DRH antenna is described in previous works [21], [22].

The conventional method for designing the shape of the reflector to produce a cosecant squared pattern in the vertical plane is GO and is described in details by many authors [5]–[8].

Doubly curved reflector antennas have two main sections. Central vertical section of the reflector must be designed to produce a shaped beam in the elevation plane. The transverse section is required to be a parabola for focusing the feed rays in the azimuth plane and consequently producing a narrow beam in that plane. The shape of the reflector antenna surface is basically determined as follows:

Referring to Fig. 1(a), Let ρ be the radius vector from F to the central vertical section curve, φ its angle of elevation, and σ the angle between the incident and reflected rays in the central vertical section. The section of the surface in the plane $OANP$ is a parabola with vertex at P and focal length

$$f(\varphi) = \rho(\varphi)\cos^2\frac{\sigma(\varphi)}{2}. \tag{1}$$

This equation gives transverse parabolas of the reflector surface [6].

The general positioning of feed-central vertical curve is shown in Fig. 1(b). Assume that the phase center of the feed is located at the focal point. As mentioned before, φ is the angle of incident ray with respect to z. θ is the angle of reflected ray. The angle between incident and reflected rays, $\sigma(\varphi)$, can be expressed as:

$$\sigma(\varphi) = \theta(\varphi) - \varphi. \tag{2}$$

The differential equation of the central curve is [5]:

$$\frac{1}{\rho}\frac{d\rho}{d\varphi} = \tan\left(\frac{\varphi-\theta}{2}\right). \tag{3}$$

In these equations, $\sigma(\varphi)$ and $\rho(\varphi)$ are both unknown. If $\sigma(\varphi)$ is specified then $\rho(\varphi)$ can be determined. The relation between θ and φ, which is necessary for integrating the above equation is as follows [5]–[8]:

$$\frac{d^2\theta}{d\varphi^2}+\left[\tan\left(\frac{\varphi-\theta}{2}\right)-\frac{I'(\varphi)}{I(\varphi)}\right]\frac{d\theta}{d\varphi}+\frac{P'(\theta)}{P(\theta)}\left(\frac{d\theta}{d\varphi}\right)^2=0 \quad (4)$$

where, $I(\varphi)d\varphi$ and $P(\theta)$ are the power incident on a central element of the reflector and the reflected energy respectively. $P(\theta)$ is required to be a $\csc^2\theta$ distribution between the angular limits θ_1 and θ_2. Finding $\theta(\varphi)$, $\sigma(\varphi)$ and $\rho(\varphi)$ will be calculated. The desired surface can be specified by combining both vertical and transverse curves of the reflector, using (1) and (3).

III. Reflector Synthesis Using IWO Algorithm

IWO is an effective numerical evolutionary optimization technique to find global optimum of complex multi-dimensional optimization problems [15]. Here IWO has been employed as a flexible method to design a doubly curved reflector antenna and achieve desired features such as low SLL and small ripples simultaneously. Other optimization algorithms, such as Genetic Algorithm (GA), Particle Swarm Optimization (PSO) and Ant Colony, are not often flexible enough to achieve desired SLL and ripple simultaneously. PSO is mainly used for sidelobe suppression [23], [24] and GA is applicable to optimize the ripple.

The algorithm process can be summarized as follows [15], [18], and [20]:

1) A finite number of seeds spread out randomly on the search area.
2) They grow to flowering weeds and produce seeds. The number of reproduced seeds of each weed depends on its own fitness, that is, better fitness permits more seeds to be reproduced. However the maximum number of seeds is limited.
3) The reproduced seeds disperse over the search area around their parent weeds. The random dispersion has a normal distribution with zero mean but varying variance. The standard deviation (SD) decreases in each time step of the algorithm as [15]:

$$SD_{iter}=\frac{(iter_{\max}-iter)^n}{(iter_{\max})^n}(SD_{initial}-SD_{final})+SD_{final} \quad (5)$$

where $iter$ is the number of current time step, $iter_{\max}$ is the maximum number of iterations, SD_{iter} is the SD at the present time step, $SD_{initial}$ and SD_{final} are prescribed constant values for SD at the first and last iterations, and n is the nonlinear modulation index usually set to 3 [15]. This decreasing behavior for SD causes aggregation of seeds around better solutions.

4) There is a maximum for number of weeds in each time step and only plants with better fitness can survive and produce seeds in the next step. The process continues until maximum number of iterations is reached and finally the plant with the best fitness is closest to the optimal solution.

In synthesis procedure based on IWO algorithm, the main idea is to find a central vertical section curve which can define a reflector profile with the desired pattern shape. Transverse sections do not affect the elevation pattern and do not need to be optimized.

In order to determine central curve using IWO algorithm, in the first step, the curve must be expressed by a finite number of parameters. For example, it can be approximated by an n-th order polynomial with $n+1$ coefficients. These coefficients are then determined properly by means of IWO. The obtained central curve along with the parabola equation given in (1), define the whole profile of the reflector. However according to (2) and (3) this curve can be obtained if the distribution of $\sigma(\varphi)$ between φ_1 and φ_2 is determined. For approximating $\sigma(\varphi)$ distribution, various functions were examined to find a function with less parameters and fine accuracy. Accordingly, the following 5-th order polynomial was chosen:

$$\sigma(\varphi)=C_0+C_1\varphi+C_2\varphi^2+C_3\varphi^3+C_4\varphi^4+C_5\varphi^5 \quad (6)$$

where $C_i, i=0,1,2,3,4,5$ are the coefficients to be determined. IWO process starts with initial random values for the coefficients in $\sigma(\varphi)$. Random central curves and then random surfaces will be generated according to (3). So in each time step of the algorithm we have a random reflector surface. To obtain elevation radiation pattern of each reflector, it has to be analyzed. Since we have the primary radiation pattern of the feed, the secondary pattern of the reflector can be obtained using the FEKO software package. The obtained elevation pattern is compared with the ideal cosecant squared pattern. Consequently, error (or fitness) value of weed (i.e., generated surface) is the difference between the far field elevation pattern and a desired cosecant squared pattern. Optimization process continues until a radiation pattern which is closest to the cosecant squared pattern is achieved.

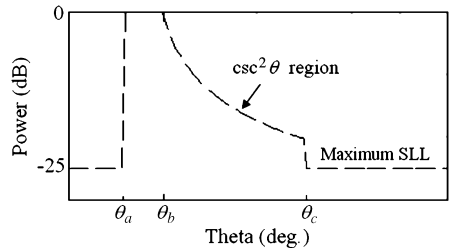

Fig. 2. Desired pattern in the shaped region and maximum level of the side lobe.

Fig. 2 presents the desired pattern in the shaped region and the maximum level of the side lobe. In the Optimization procedure, the focus is on achieving low ripples in shaped region and the desired SLL which is defined to be -25 dB (lower values can be defined). To do this it is required to calculate a proper fitness function for every generated reflector to define the shaped region error. Consider that the obtained elevation pattern of each reflector varies from -180° to 180°. By sampling the radiated power $P(\theta)$ at k points of this pattern, a fitness function is defined as:

$$f=\frac{1}{k}\left(\sum_{i=1}^{m}\left(\left|P(\theta_i)-\csc^2\theta\right|\right)^2+\sum_{i=m+1}^{k}\left(\frac{1}{2}\left(X_i+|X_i|\right)\right)^2\right) \quad (7)$$

where

$$X_i=\left[P(\theta_i)-(-25)\right], \quad 1<m<k$$

The first term with m sample points in the fitness function is the error due to ripples in the shaped region ($\theta_b \le \theta \le \theta_c$) and the second term is the relative error of the desired SLL ($-180 \le \theta \le \theta_a, \theta_c \le \theta \le 180$). So that beyond 25 SLL, the error is not accounted. The region between θ_a and θ_b does not affect the total error.

IV. Results and Discussion

A. DRH Antenna Feed

The performance of the designed pyramidal DRH antenna was checked by simulation using Ansoft HFSS and CST Microwave Studio and then by measurement. It was fabricated with high precision (mechanical tolerance of 0.1 mm). Fig. 3(a) shows a picture of the fabricated antenna.

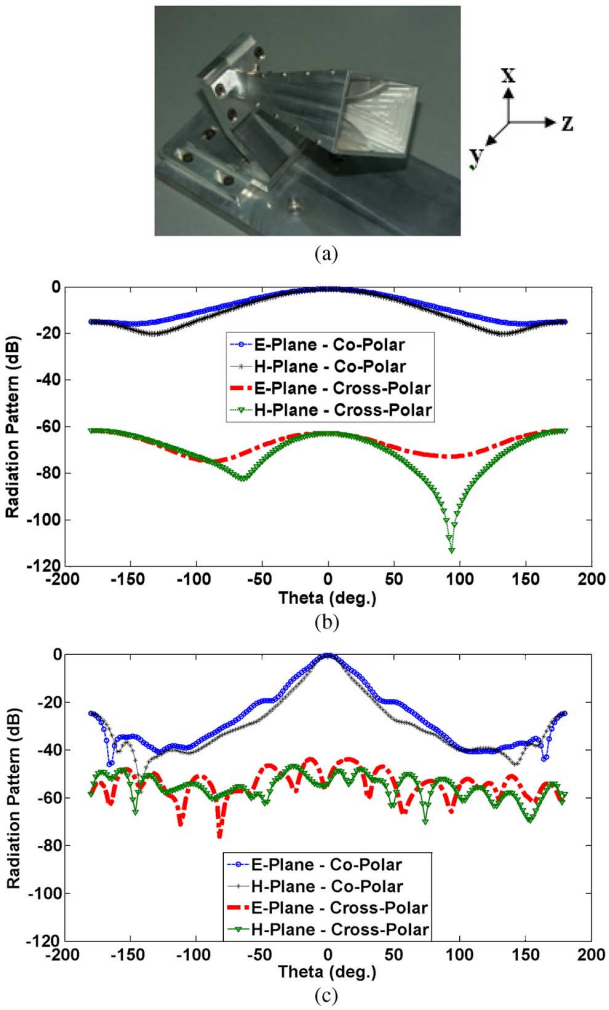

Fig. 3. (a) Picture of the fabricated DRH antenna, (b), (c) Measured radiation patterns of the DRH antenna at 2 GHz and 18 GHz.

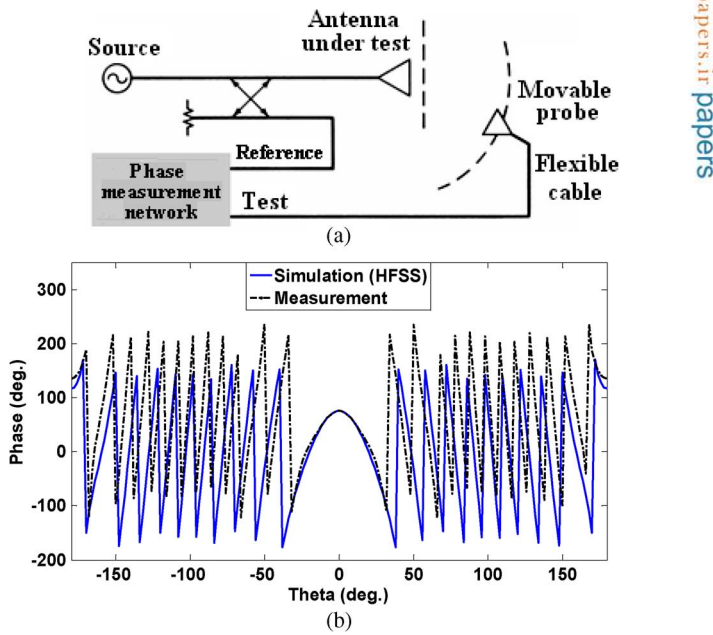

Fig. 4. (a) Near-field phase pattern measuring system, (b) Simulated and measured phase patterns of the DRH at 10 GHz.

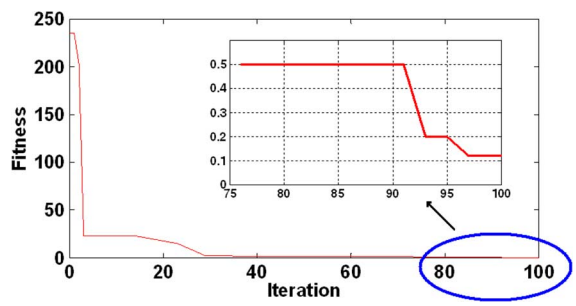

Fig. 5. Convergence curve of the fitness function.

The measured co- and cross polar far-field E-plane (x-z plane) and H-plane (y-z plane) radiation patterns of the designed feed horn at band edge frequencies are presented in Fig. 3(b) and (c). In this figure, for the E-plane, E_θ-field and E_ϕ-field are co-polar and cross-polar components, respectively. For the H-plane, E_ϕ-field and E_θ-field are co-polar and cross-polar components, respectively. It can be observed that the proposed feed has symmetrical radiation patterns and low SLL over the entire frequency band. Specifically, the cross polarization level at boresight direction is considerably small.

The basic system that is used to measure the phase patterns at a short distance from the antenna is shown in Fig. 4(a) [25]. The phase of the received signal is compared with a coupled input signal as the reference. Comparison of simulated and measured phase patterns of the DRH at the center frequency is presented in Fig. 4(b). The smooth variation of this phase pattern in illumination angle is of significance in the design of the shaped reflector.

B. Complete Reflector Antenna System

Numerous simulations via MATLAB and FEKO software packages have been made to optimize the performance of the reflector antenna system.

The IWO parameters are chosen as: $iter_{\max} = 100$, $k = 50$, $SD_{initial} = 10$, and $SD_{final} = 0.2$. Since the feed is placed with 15° offset and has about 56° 10-dB beam width at the center frequency (10 GHz), φ varies from $-13°$ to 43°. $\sigma(\varphi)$ is approximated according to (6). Fig. 5 shows convergence curve of the fitness function. After 100 iterations, lowest fitness and consequently the optimum solution is achieved. The final optimum values of C_i, $i = 0, 1, 2, 3, 4, 5$ are tabulated in Table I.

TABLE I
FINAL OPTIMUM VALUES OF THE COEFFICIENTS OF $\sigma(\varphi)$

coefficient	C_0	C_1	C_2	C_3	C_4	C_5
value	0.1508	-0.2374	0.4079	0.2562	-0.1522	0.1486

Since the primary radiation pattern of the feed is known, we obtain the secondary pattern of the generated reflectors using FEKO software package. The far filed patterns of the obtained surfaces at the center frequency are shown in Fig. 6. The dashed line in this figure represents the desired defined goal for elevation pattern used to calculate the fitness function. It can be observed that the obtained patterns approach to the defined goal as the number of iteration increases.

The 3D model of the complete designed reflector antenna system is presented in Fig. 7. The antenna dimension and the focal length are $50 \times 50\ \mathrm{cm}^2$ and 44 cm respectively. As mentioned before, the placement of the horn is such that its phase center is at the focal point of the reflector. The angular limits φ_1, φ_2 of the designed reflector correspond to the 10-dB points in the primary pattern at 10 GHz.

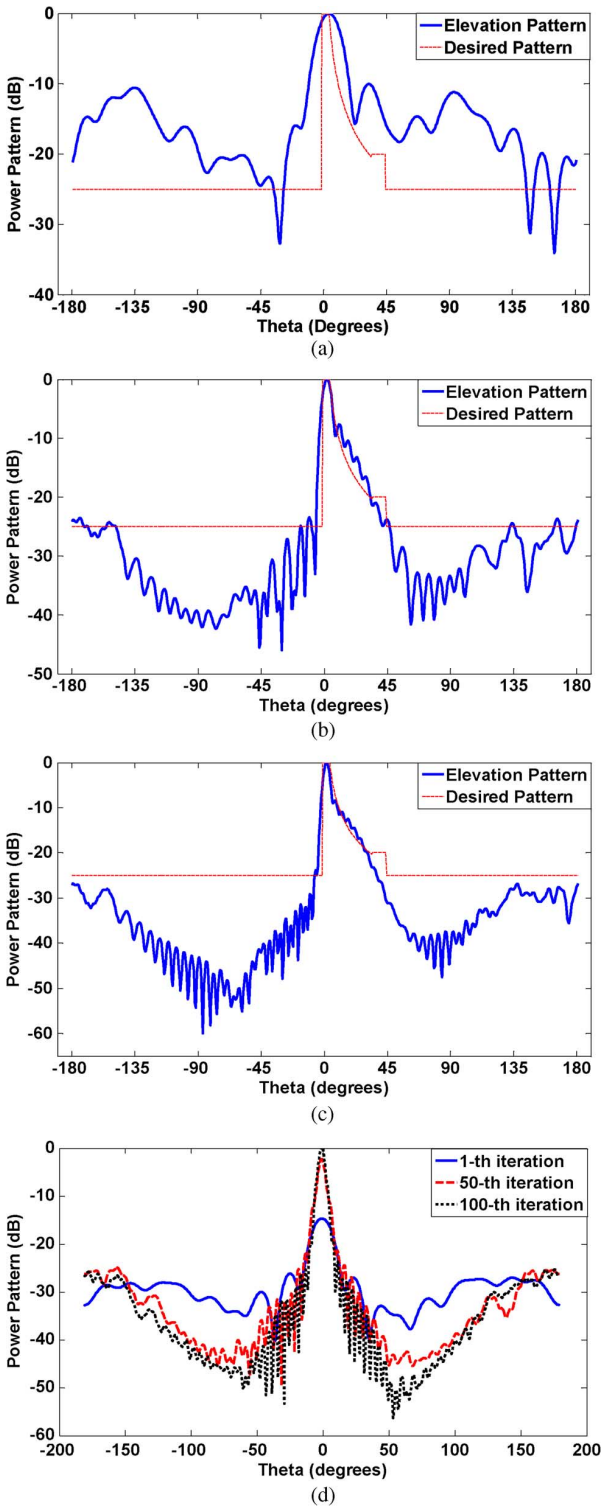

Fig. 6. Radiation patterns of generated reflector surfaces, (a) elevation pattern in the first iteration, (b) elevation pattern in the 50-th iteration, (c) elevation pattern of the final optimum reflector surface generated in the 100-th iteration, (d) azimuth patterns.

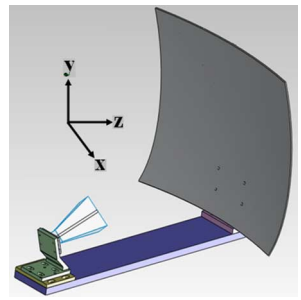

Fig. 7. 3D model of the complete reflector antenna system.

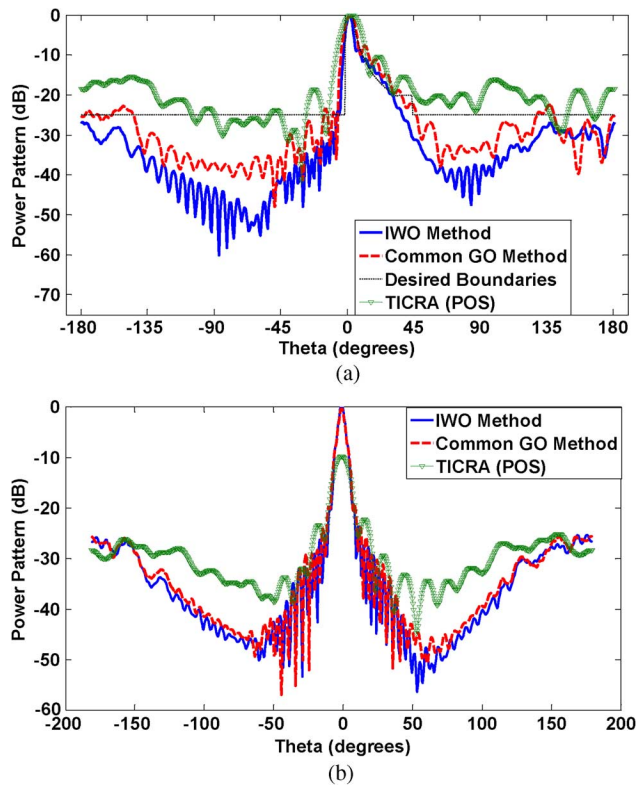

Fig. 8. A comparison between the IWO, common GO based method, and TICRA tool results. (a) elevation pattern, (b) pencil beam in the azimuth pattern.

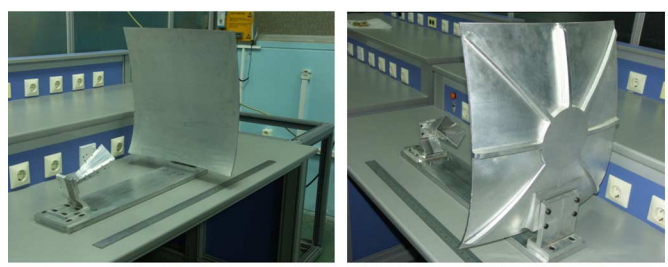

Fig. 9. Pictures of the fabricated antenna, (a) overall view, (b) back view.

In order to compare the proposed method with the common GO based method and TICRA CAD tool, the reflector surface is designed in identical conditions, that is the same feed position, reflector dimensions and bandwidth. TICRA package supplies physical optics-based shaped reflector (POS) code which provides accurate and efficient shaping of spacecraft antennas [26]. The resulted radiation patterns obtained by three methods are depicted in Fig. 8. It is seen that the ripple in the cosecant squared region for the designed antenna using IWO method, is <1.5 dB, but the patterns obtained by other methods have considerably larger ripples. Moreover, the IWO based design has a lower SLL. The inferior performance of the TICRA tool can be due to the fact that it is not efficient for broadband shaped reflector design.

Finally, the designed reflector antenna system was fabricated with a mechanical accuracy of 0.01λ and tested. Fig. 9 shows the pictures of the fabricated antenna. As shown in this figure, in order to achieve the

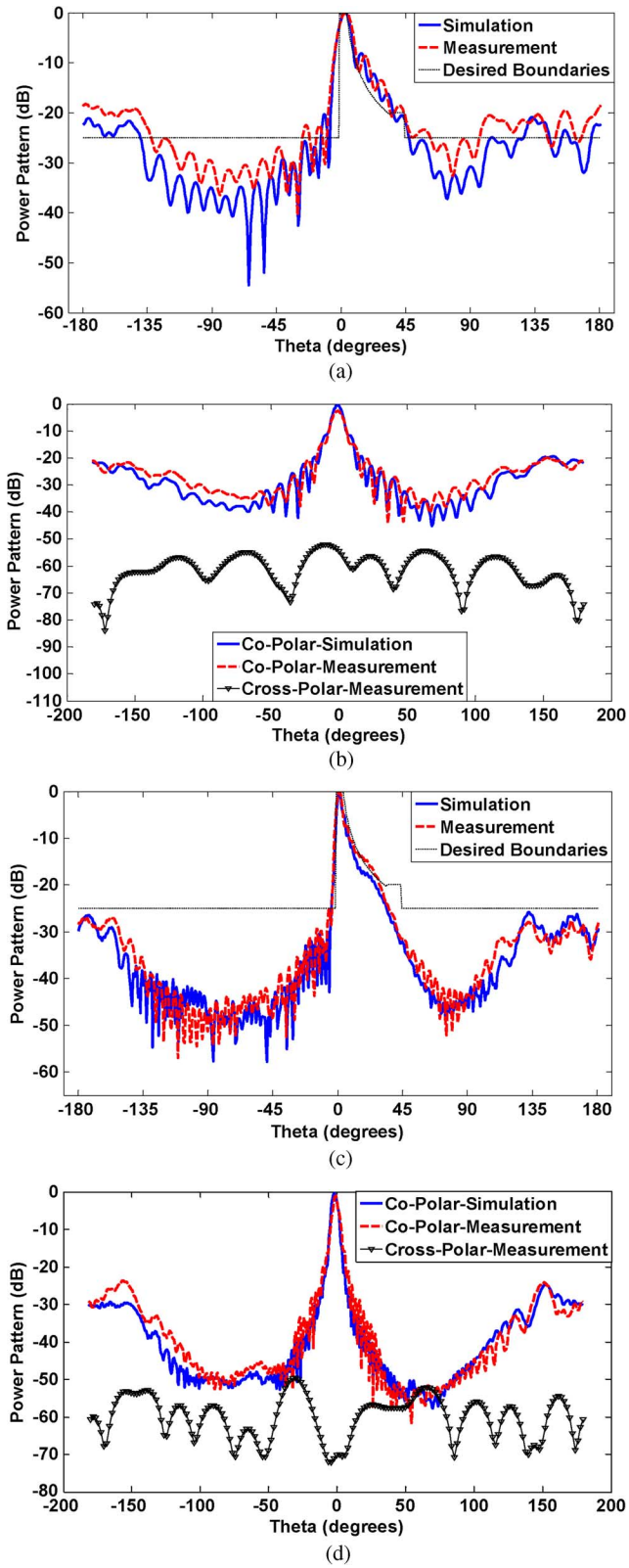

Fig. 10. Simulated and measured far-filed patterns of the designed antenna, (a) elevation pattern at 2 GHz, (b) azimuth pattern at 2 GHz, (c) elevation pattern at 18 GHz, (d) azimuth pattern at 18 GHz.

slant polarization performance, the feed horn antenna is located at 45° azimuthally slanted position.

The simulated and measured far-filed patterns of the designed antenna at band edge frequencies are presented in Fig. 10. It can be observed that the designed antenna has satisfactory radiation patterns with low ripple in the cosecant squared region and low SLL over the entire frequency band. Moreover, the designed reflector antenna has a cross polarization level about 50 dB lower than the co-polarization level at boresight in all of the measured radiation patterns.

TABLE II
MEASURED GAIN, RIPPLE AND SLL OF THE REFLECTOR ANTENNA VERSUS FREQUENCY

Frequency (GHz)	2	6	10	14	18
Max. gain (dB)	23.3	25.5	27.4	28.6	30.1
Ripple (dB)	1.5	1.3	0.9	0.7	0.5
SLL (dB)	-19.3	-23.6	-24.5	-26.2	-27.4

The angular width of the $\csc^2\theta$ distribution is approximately 45° and depends on the 10-dB points in the primary pattern and initial value of $d\theta/d\varphi$ in (4). The gain, ripple, and the SLL variations of the reflector with frequency are presented in Table II. It can be seen that the gain of the antenna increases as frequency increases. The antenna peak gain is about 30 dB and occurs at the end of the frequency band (18 GHz). The reflector antenna has smaller ripples and lower SLL at higher frequencies.

The effect of blocking by the primary feed in the radiation pattern is eliminated by the offset feeding technique. As illustrated schematically in Fig. 1(b), the feed is placed with 15° offset. This avoids the shadow of the horn and its supporting structure on the most intensely illuminated area of the reflector and hence improves gain and side lobe characteristics [6]. The agreement between the simulations and measurements confirms this point.

V. CONCLUSION

Based on GO analysis, IWO algorithm has been successfully employed for design and optimization of a 2–18 GHz doubly curved reflector antenna. Simulation results have been checked experimentally and excellent agreement is obtained. It was found that for satisfactory antenna performance, high mechanical accuracy and small geometrical tolerances of the feed horn and reflector are essential. In this communication the focus is on lower ripples in the cosecant squared region and low SLL. The designed reflector based on the IWO method is compared with other reflectors designed using common GO method and TICRA software package. It is shown that improved performance is obtained using IWO method. The proposed reflector antenna can be used in broadband surveillance-search radar systems, ground-mapping radars, and airport beacons.

REFERENCES

[1] A. Brunner, "Possibilities of dimensioning doubly curved reflectors for azimuth-search radar antennas," *IEEE Trans. Antennas Propag.*, vol. 19, no. 1, Jan. 1971.
[2] T. F. Carberry, "Analysis theory for the shaped-beam doubly curved reflector antenna," *IEEE Trans. Antennas Propag.*, vol. 17, no. 2, Mar. 1969.
[3] C. F. Winter, "Dual vertical beam properties of doubly curved reflectors," *IEEE Trans. Antennas Propag.*, vol. 19, no. 2, Mar. 1971.
[4] S. Karimkashi, A. R. Mallahzadeh, and J. Rashed-Mohassel, "A new shaped reflector antenna for wide beam radiation patterns," in *Proc. IEEE Int. Symp. on Microwave, Antenna, Propagation, and EMC Technologies for Wireless Communications*, Aug. 2007, pp. 535–538.
[5] A. S. Dunbar, "Calculation of doubly curved reflectors for shaped beams," *Proc. IRE*, vol. 36, pp. 1289–1290, Oct. 1948.
[6] S. Silver, *Microwave Antenna Theory and Design*. New York, NY, USA: McGraw-Hill, 1949.
[7] R. S. Elliott, *Antenna Theory and Design*. New York, NY, USA: Wiley, 2003.
[8] T. A. Milligan, *Modern Antenna Design*, 2nd ed. Hoboken, NJ, USA: John Wiley, 2005.

[9] D. W. Duan and Y. Rahmat-Samii, "A generalized diffraction synthesis technique for high performance reflector antennas," *IEEE Trans. Antennas Propag.*, vol. 43, no. l, Jan. 1995.

[10] E. L. Holzman, "Pillbox antenna design for millimeter-wave base-station applications," *IEEE Antennas Propag. Mag.*, vol. 45, no. 1, Feb. 2003.

[11] J. Sletten, "Ray tracing method for doubly curved reflector surfaces," *Proc. IEEE*, vol. 69, no. 6, pp. 743–744, Jun. 1981.

[12] S. L. Avila, W. P. Carpes, Jr., and J. A. Vasconcelos, "Optimization of an offset reflector antenna using genetic algorithm," *IEEE Trans. Magn.*, vol. 40, no. 2, Mar. 2004.

[13] J. Martinez-Fernandez, J. M. Gil, and J. Zapata, "Ultrawideband optimized profile monopole antenna by means of simulated annealing algorithm and the finite element method," *IEEE Trans. Antennas Propag.*, vol. 55, no. 6, pp. 1826–1832, Jun. 2007.

[14] S. Alfonzetti, G. Borzì, E. Dilettoso, and N. Salerno, "Stochastic optimization of a patch antenna," *ACES J.*, vol. 23, no. 3, pp. 237–242, Sept. 2008.

[15] A. R. Mehrabian and C. Lucas, "A novel numerical optimization algorithm inspired from weed colonization," *Ecol. Inf.*, vol. 1, pp. 355–366, 2006.

[16] A. R. Mallahzadeh, H. Oraizi, and Z. Davoodi-Rad, "Application of the invasive weed optimization technique for antenna configurations," *Progr. Electromagn. Res., PIER*, vol. 52, pp. 225–254, 2008.

[17] A. R. Mallahzadeh, S. Es'haghi, and H. R. Hassani, "Compact U-array MIMO antenna designs using IWO algorithm," *Int. J RF Microw. CAE*, vol. 19, no. 5, pp. 568–576, Sep. 2009.

[18] S. Pal, A. Basak, S. Das, and A. Abraham, "Linear antenna array synthesis with invasive weed optimization algorithm," in *Proc. Int. Conf. on Soft Computing and Pattern Recognition (SoCPaR)*, Dec. 2009, pp. 161–166.

[19] B. Bahreini, A. R. Mallahzadeh, and M. Soleimani, "Design of a meander-shaped MIMO antenna using IWO algorithm for wireless applications," *ACES J.*, vol. 25, no. 7, pp. 631–638, Jul. 2010.

[20] A. R. Mallahzadeh and P. Taghikhani, "Cosecant squared pattern synthesis for reflector antenna using a stochastic method," *ACES J.*, vol. 26, no. 10, pp. 823–830, Oct. 2011.

[21] A. R. Mallahzadeh, A. A. Dastranj, and H. R. Hassani, "A novel dual-polarized double-ridged horn antenna for wideband applications," *Progr. Electromagn. Res. B*, vol. 1, pp. 67–80, 2008.

[22] A. A. Dastranj, H. Abiri, and A. R. Mallahzadeh, "Design of conical DRH antennas for K and Ka frequency bands," *Int. J. RF Microw. CAE*, vol. 21, no. 5, pp. 602–610, Sep. 2011.

[23] Y. R. Samii and N. B. Jin, "Particle swarm optimization (PSO) in engineering electromagnetics: A nature-inspired evolutionary algorithm," in *Proc. IEEE Int. Conf. on Electromagnetics in Advanced Application*, 2007, pp. 177–182, ICEAA.

[24] X. M. Zhang, K. M. Luk, X. Bai, Y. H. Wang, and J. Y. Li, "Ultra-low sidelobe synthesis of non-uniformly linear array antennas by particle swarm optimization," *PIERS*, pp. 1302–1305, 2008.

[25] C. A. Balanis, *Antenna Theory: Analysis and Design*, 2nd ed. New York, USA: Wiley, 1997.

[26] [Online]. Available: www.TICRA.com

Sidelobe Modulation Scrambling Transmitter Using Fourier Rotman Lens

Yunhua Zhang, Yuan Ding, and Vincent Fusco

***Abstract*—A means for scrambling the digital modulation content in the sidelobes of a radio transmission from a steerable antenna array is presented. The method uses a Fourier transform beam-forming network simultaneously excited by an RF information stream and orthogonally injected interference streams. The proposed system is implemented using a Fourier Rotman lens and its operational characteristics are validated for a 10 GHz QPSK transmission.**

***Index Terms*—Fourier transform beamforming, physical layer security, Rotman lens.**

I. Introduction

The demand for high level secure wireless communication systems is an imperative [1]. In addition to encryption imposed at application layers the adoption of physical layer security techniques can add more challenges to eavesdropper attempts to intercept and successfully decipher useful information. Recently several physical-layer spatial encryption technologies have been proposed [2]–[8]. Here physical layer data security is realized by distorting the IQ plane constellation diagram of the transmitted signal in all spatial directions except along a pre-specified direction in order to hamper data decoding in all directions except the pre-specified one.

In [2] and [3], spatial data encryption is achieved for phase and amplitude modulated signals respectively by transversely placing active phase conjugating lens (or lenses) between transmitters and receivers. However, the frequency bandwidth of modulated signals is limited by the inherent narrow bandwidth of analog phase conjugating lenses. Furthermore, the secure communication direction cannot be scanned except by mechanically rotating the system. Other physical-layer spatial encryption technologies, under the banner of directional modulation (DM), have been suggested in [4]–[8]. To date DM systems have been implemented by using passive parasitic arrays [4], [5] or actively driven arrays of phased antennas [6]–[8]. In both methods the transmission phase characteristics of each element in the radiating array is updated on a symbol-by-symbol basis. Consequently symbol encoding is extremely demanding from an RF design perspective, since the use of multiple RF switches and digital phase shifters poses a major complexity challenge.

A Fourier transform based beam-forming network (FT-BFN), such as a Butler matrix [9], [10] has the capability to simultaneously produce multiple beams which are orthogonal in the beam space. In the

Manuscript received November 09, 2012; revised March 15, 2013; accepted March 16, 2013. Date of publication March 22, 2013; date of current version July 01, 2013. This work was supported in part by the Queen's University of Belfast High Frequency Research Scholarship and in part by the UK Engineering and Physical Research Council under Grant EP/H049606/1.

Y. Zhang was with the Institute of Electronics, Communications and Information Technology (ECIT), Queen's University of Belfast, Belfast BT3 9DT, U.K. He is now with the School of Electronic Information, Wuhan University, Wuhan 430072, China (e-mail: zhangyunhuawhu@hotmail.com).

Y. Ding and V. Fusco are with the Institute of Electronics, Communications and Information Technology (ECIT), Queen's University of Belfast, Belfast BT3 9DT, U.K. (e-mail: yding03@qub.ac.uk; v.fusco@qub.ac.uk).

Color versions of one or more of the figures in this communication are available online at http://ieeexplore.ieee.org.

Digital Object Identifier 10.1109/TAP.2013.2254453